

## Observational Study



# Altered Neurovascular Coupling in Patients with Chronic Myofascial Pain

Ganjun Song, MD<sup>1,2</sup>, Yonghan Zhang, MD<sup>2</sup>, Bangyong Qin, MD<sup>3</sup>, Junwei Zeng, PhD<sup>4</sup>,  
Tijiang Zhang, MD, PhD<sup>1</sup>, and Peng Xie, MD, PhD<sup>2</sup>

From: <sup>1</sup>Department of Radiology, Affiliated Hospital of Zunyi Medical University, Zunyi, Guizhou, China; <sup>2</sup>Department of Critical Care Medicine, the Third Affiliated Hospital (The First People's Hospital of Zunyi) of Zunyi Medical University, Zunyi, Guizhou, China; <sup>3</sup>Department of Pain Medicine, Affiliated Hospital of Zunyi Medical University, Zunyi, Guizhou, China; <sup>4</sup>Department of Physiology, Zunyi Medical University, Zunyi, Guizhou province, China

Address Correspondence:  
Peng Xie, MD, PhD  
Department of Critical Care Medicine,  
the Third Affiliated Hospital (The First  
People's Hospital of Zunyi) of Zunyi  
Medical University, Feng Huang Road  
98, Huichuan Distric, Zunyi, Guizhou  
Province, China  
E-mail: pxie@zmu.edu.cn

Disclaimer: G Song and Y Zhang  
contributed equally to the work and  
should be regarded as co-first authors.

This work was supported by the  
National Natural Science Foundation  
(Grant No.31660290) of China.

Conflict of interest: Each author  
certifies that he or she, or a member  
of his or her immediate family, has  
no commercial association (i.e.,  
consultancies, stock ownership,  
equity interest, patent/licensing  
arrangements, etc.) that might pose a  
conflict of interest in connection with  
the submitted manuscript.

Manuscript received: 06-30-2020  
Revised manuscript received:  
11-05-2020  
Accepted for publication:  
12-08-2020

Free full manuscript:  
[www.painphysicianjournal.com](http://www.painphysicianjournal.com)

**Background:** Despite previous reports on cerebral structures and functional connectivity in patients with myofascial pain (MFP), it is not clear whether alterations in neurovascular coupling occur in these patients.

**Objectives:** We analyzed the coupling between resting-state cerebral blood flow (CBF) and functional connectivity strength (FCS) for observation of neurovascular coupling in patients with chronic MFP.

**Study Design:** Observational study.

**Setting:** University hospital.

**Methods:** Resting-state functional magnetic resonance imaging and arterial spin labeling were performed in 23 patients with chronic MFP and 23 healthy controls (HC) for the calculation of FCS and CBF. The whole-brain gray matter CBF-FCS correlations and CBF/FCS ratios of the various voxels of the 2 groups were subsequently compared.

**Results:** Compared with the HC, the patients with MFP experienced a decrease in whole-brain gray matter CBF-FCS coupling. In patients with MFP, a decrease in CBF/FCS was found in the bilateral superior temporal gyri, right parahippocampal gyrus, right hippocampus, caudate nucleus, right medial prefrontal cortex, and the periaqueductal gray matter (PAG), whereas an increase in CBF/FCS was found in the bilateral lingual gyri, posterior cingulate cortex, and bilateral inferior parietal lobules. In addition, the CBF/FCS of the PAG in patients with MFP was significantly negatively correlated with the pain visual analog scale score and pain duration.

**Limitations:** Alterations in neurovascular coupling in patients with MFP were observed only before treatment. Therefore, there is a lack of data on the alterations that occurred after treatment.

**Conclusion:** This study demonstrated for the first time that impairment of neurovascular coupling in the brain may be a potential neuropathological mechanism of chronic MFP.

**Key Words:** Myofascial pain, resting-state functional magnetic resonance imaging, arterial spin labeling, cerebral blood flow, functional connectivity strength, neurovascular coupling.

**Pain Physician 2021; 24:E601-E610**

**M** yofascial pain syndrome (MFPS) is a chronic musculoskeletal pain disorder mainly characterized by the presence of active myofascial trigger points (MTrPs), which elicit local or referred pain accompanied by local twitch responses in muscles upon compression (1). At

present, there is no standard treatment regimen for MFP, with traditional treatment methods providing unsatisfactory therapeutic effects (2). Consequently, the pain frequently recurs, leading to increasingly severe chronic pain (3-5) and resulting in considerable psychological and economic burdens on patients and society. Although it is generally believed that the pathogenesis of MFP may be related to peripheral and central sensitization, the exact mechanisms remain unclear (6).

Many neuroimaging studies have shown that chronic pain not only causes abnormalities in brain structure and function but also induces alterations in cerebral blood flow (CBF) (7-10). Our previous study and other relevant reports have also confirmed the presence of abnormalities in the gray matter microstructure and brain functional connectivity of patients with MFP (11,12). However, it is not known whether alterations occur in the coupling between resting-state CBF and functional connectivity in patients with MFP. Functional connectivity strength (FCS), which is based on graph theory analysis, enables the unbiased observation of voxel-wise whole-brain functional connectivity and reflects the importance of brain regions or nodes in whole-brain functional networks (13). It is also closely linked to local CBF and glucose metabolism (14,15).

Previous research has indicated that CBF is closely associated with resting-state brain metabolism (16), with both CBF and glucose metabolism increasing in proportion during functional activation (17,18). Neurovascular units (NVUs), which form the structural basis of neurovascular coupling, are complete functional units mainly composed of neurons, vascular cells, and glial cells (19,20). Damage to any of the components of the NVUs may influence their function and result in neurovascular coupling abnormalities (21). According to the neurovascular coupling theory, brain regions with stronger connectivity have higher spontaneous neuronal activity, which requires higher energy consumption and leads to increased perfusion (15,22). In addition, previous studies have proven that brain connectivity is related to CBF and that the across-voxel CBF-FCS correlation and CBF/FCS ratio can be used to characterize the coupling between neuronal activity and vascular responses (14,23).

Here, we aimed to observe whether the neurovascular coupling changes in patients with MFP, and whether this change was related to pain intensity and duration.

## METHODS

### Study Patients

This study was approved by a local research ethics committee (Ethical Application Ref: [2016] 1-007), and all patients and their family members signed an informed consent form prior to study inclusion. Twenty-three patients with chronic MFP aged 22-48 years were recruited from local outpatient pain management clinics. All patients were dextrorhous, fulfilled the diagnostic criteria for MFPS (1,11), and were diagnosed by pain management specialists with at least 10 years of experience in MFPS diagnosis and treatment.

Inclusion criteria were 1) palpable stiff or hardened nodules in the left trapezius muscle; 2) aggravated pain or referral of pain to a distant site during MTrP palpation, with rapid compression possibly inducing local twitch responses and pain becoming aggravated under conditions of mental strain or insufficient sleep; 3) pain lasting for more than 3 months, visual analog scale (VAS) score  $\geq 5$ ; (4) no previous treatment or use of nonsteroidal anti-inflammatory drugs, acetaminophen, or antipsychotics. Exclusion criteria were 1) a history of other chronic pain conditions; 2) a history of trauma, surgery, shoulder joint dislocation, or rheumatism; 3) systemic disease or central nervous system disorder; 4) contraindications for magnetic resonance imaging (MRI); 5) presence of distinct organic lesions as shown by MRI scans; 6) pregnancy, intellectual disability, or mental or emotional disorder; 7) body mass index  $> 30$  kg/m<sup>2</sup>.

The healthy controls (HC) group consisted of 23 dextrorhous volunteers with age, gender, and educational levels comparable to those of the patients with MFP. The absence of a history of chronic pain and potential MTrPs in the trapezius muscles of the HC were confirmed through screening by pain management specialists, and the exclusion criteria for the HC were identical to that of the MFP group.

### fMRI Data Acquisition

All MRI data were acquired using a Signa HDxt 3.0T MRI scanner with an 8-channel phased-array head coil (GE Healthcare, Chicago, IL). An MR-compatible foam positioner was used for head fixation. During the scanning process, patients were requested to keep their eyes closed, stay awake and relaxed, and use ear plugs for noise reduction. To exclude patients with intracranial organic lesions, routine T2-weighted fluid-attenuated inversion recovery scans were performed using the following sequence parameters: repetition

time (TR), 7,000 milliseconds; echo time (TE), 93 milliseconds; field of view (FOV), 240 mm × 240 mm; matrix, 320 × 320; number of excitations (NEX), 2; number of slices, 20; slice thickness, 5 mm; slice spacing, 1.5 mm; scan duration, 97 seconds. Sequence parameters for resting-state blood oxygen-level-dependent fMRI (rs-BOLD-fMRI) were as follows: TR, 2,000 milliseconds; TE, 30 milliseconds; FOV, 240 mm × 240 mm; matrix, 64 × 64; number of slices, 33; slice thickness, 5 mm; slice spacing, 0 mm; scan duration, 413 seconds. A total of 6,930 images were acquired across 210 time points.

The sequence parameters for 3-dimensional pseudo-continuous arterial spin labeling (3D-pcASL) were as follows: TR, 4599 milliseconds; TE, 9.8 milliseconds; FOV, 240 mm × 240 mm; number of sampling points, 512; number of spiral arms, 8; NEX, 3; slice thickness, 4 mm; slice spacing, 0 mm; scan duration, 267 seconds. Parameters for 3D T1-weighted structural imaging (T1WI) were as follows: TR, 7.8 ms; TE, 3 ms; matrix, 256 × 256; FOV, 256 mm × 256 mm; NEX, one; slice thickness, one mm; slice spacing, 0 mm; bandwidth, 31.25 Hz; flip angle, 12°; inversion time, 450 milliseconds.

### CBF Analysis

CBF was evaluated using previously described methods (24,25). In brief, we corrected for head motion, removed nonbrain voxels, and acquired CBF images using a 3D-pcASL sequence. The CBF images in each patient's structural space were then transformed to a Montreal Neurological Institute (MNI) standard space. Subsequently, nonbrain tissue was excluded from the normalized CBF images, and the CBF values of each patient were normalized by dividing the voxel-wise CBF values by the whole-brain averaged CBF value. Finally, all CBF images were smoothed using an 8 mm × 8 mm × 8 mm full-width half-maximum (FWHM) Gaussian kernel filter.

### FCS Analysis

The rs-BOLD fMRI data were preprocessed using the Statistical Parametric Mapping 8 (SPM8) software package. First, data of the first 10 time points were deleted, and the following preprocessing steps were sequentially performed: timing difference correction, head motion correction, regression of covariates, band-pass filtering (frequency: 0.01–0.08 Hz), spatial normalization, and spatial smoothing. The preprocessed data were then subjected to voxel-wise whole-brain resting-state FCS analysis. The correlation coefficients (*r* values) of the gray-matter voxels for all time series were calculated and converted to *z* values. For each voxel, the

FCS value was computed by summing the connectivities between the voxel and all other gray-matter voxels across the whole brain. To eliminate weak correlations caused by noise, a threshold value of  $r = 0.2$  was used. Lastly, spatial smoothing was performed on the FCS images using an 8 mm × 8 mm × 8 mm FWHM Gaussian kernel filter.

### Whole-brain Gray Matter Image Analysis

The raw 3D T1WI structural images in Digital Imaging and Communications in Medicine (DICOM) format were converted to Neuroimaging Informatics Technology Initiative (NIFTI) files, and the origin in the images of each patient was manually corrected to coincide with the anterior commissure in the MNI coordinate system. Using SPM8, the 3D T1WI images were segmented into gray matter, white matter, and cerebrospinal fluid images. The segmented gray matter images were initialized in the Diffeomorphic Anatomical Registration Through Exponentiated Lie Algebra (DARTEL) tool and normalized using the DARTEL algorithm. Six templates and deformation fields were generated after 18 iterations, and the sixth template and deformation field, which achieved the highest accuracy, were used for the normalization of all gray matter to the standard MNI space. Finally, the modulated gray matter images were smoothed using an 8 mm × 8 mm × 8 mm FWHM Gaussian kernel filter.

### Whole-brain Gray Matter CBF-FCS Coupling Analysis

To quantitatively evaluate the coupling relationship between CBF and FCS, across-voxel correlation analysis within the gray matter template was performed to obtain the CBF-FCS correlation coefficient for each patient. The independent-samples *t*-test was then used to compare the difference in CBF-FCS correlation coefficients between the 2 groups.

### CBF/FCS Ratio Analysis

To quantitatively evaluate neurovascular coupling in the patients, the value of the CBF/FCS ratio for each voxel within the gray matter template was calculated and normalized. A voxel-wise independent-samples *t*-test was then performed to determine the brain regions with significant intergroup differences in the CBF/FCS ratio, with age, gender, and education level used as covariates during the comparison. *P* values were adjusted for multiple comparisons using the false discovery rate (FDR) correction.

### Voxel-wise Comparisons of CBF and FCS

To compare the differences between CBF/FCS ratio analysis and CBF or FCS analysis and to further elucidate the alterations in neurovascular coupling, a voxel-wise independent-samples t-test was performed to compare the differences in CBF and FCS between the 2 groups while controlling for the influences of age, gender, and education level. A voxel-wise FDR correction was performed for the adjustment of P values for multiple comparisons.

### Validation Analysis

Previous studies have reported the presence of gray matter alterations in patients with chronic MFP (10,11). To reduce the possible influence of local gray matter volume (GMV) alterations on neurovascular coupling and validate the reliability of our results, we extracted the whole-brain GMV data of all patients and performed repeated voxel-wise intergroup comparisons of the CBF/FCS ratios while controlling for the influence of age, gender, education level, and whole-brain GMV values.

### Statistical Analysis

Statistical analysis of demographic and clinical data was performed using SPSS 18.0 (SPSS Inc., Chicago, IL). The  $\chi^2$  test was used for gender data, whereas differences between the 2 groups for all other variables were compared using the independent-samples t-test. Spearman's rank correlation coefficient was used to measure the correlations between the CBF/FCS ratios with significant intergroup differences and clinical data.  $P < 0.05$  was considered significant.

## RESULTS

### Demographic and Clinical Data

Clinical characteristics of patients with MFP and HC are listed in Table 1. There were no significant differences in age ( $t = 1.14$ ,  $P = 0.26$ ), gender ( $\chi^2 = 0.35$ ,  $P = 0.77$ ), and education level ( $t = 1.09$ ,  $P = 0.28$ ) between the patients with chronic MFP and HC.

### Spatial Distributions of CBF, FCS, and CBF/FCS

The spatial distributions of CBF, FCS, and CBF/FCS of the MFP and HC were similar. The brain regions with high CBF, FCS, and CBF/FCS values mainly included the medial prefrontal cortex, cingulate cortex, temporal lobe, parietal lobe, occipital lobe, and thalamus (Fig. 1).

### Alterations in CBF-FCS Coupling in Whole-brain Gray Matter of Patients with MFP

A significant voxel-wise correlation existed between CBF and FCS in both the patients with MFP and HC groups (Fig. 2A). In the patients with MFP group, the whole-brain gray matter CBF-FCS coupling was decreased significantly compared with that of the HC ( $t = 2.221$ ,  $P = 0.0296$ ) (Fig. 2B).

### Alterations in the CBF/FCS Ratios of Patients with MFP

Compared with the HC, the patients with MFP group had decreased CBF/FCS ratios in the bilateral superior temporal gyri, right parahippocampal gyrus, right hippocampus, caudate nucleus, right medial prefrontal cortex, and periaqueductal gray matter (PAG) and increased CBF/FCS ratios in the bilateral lingual gyri, posterior cingulate cortex, and bilateral inferior parietal lobules (Fig. 3 and Table 2,  $P < 0.05$ , FDR-corrected).

### Alterations in CBF and FCS of Patients with MFP

Compared with the HC, the patients with MFP group had decreased CBF values in the bilateral superior temporal gyri, left middle temporal gyrus, medial frontal gyrus, right middle frontal gyrus, and PAG; increased CBF values in the right inferior temporal gyrus, left calcarine gyrus, and left parahippocampal gyrus (Fig. 4 and Table 3,  $P < 0.05$ , FDR-corrected); decreased FCS values in the left lingual gyrus, right superior frontal gyrus, left insula, and left inferior parietal lobule; and increased FCS values in the right superior temporal gyrus, right parahippocampal gyrus, left middle temporal gyrus, left superior frontal gyrus, and PAG (Fig. 5 and Table 4,  $P < 0.05$ , FDR-corrected).

### Correlations between CBF/FCS Ratios and Clinical Data of Patients with MFP

The CBF/FCS ratios of brain regions in patients with MFP that differed significantly from the corresponding ratios of the HC were extracted for the analysis of the correlations of these ratios with the VAS and pain duration of these patients. Results indicated that the CBF/FCS ratio of the PAG in patients with MFP was significantly negatively correlated with VAS and duration of pain ( $P < 0.05$ , Table 5).

### Validation Analysis

As GMV atrophy may influence neurovascular cou-

Table 1. Demographic and clinical characteristics of the MFP and HC.

Characteristics	MFP (n = 23)	HC (n = 23)	Statistics	P values
Gender (M/F)	12/11	10/13	$\chi^2 = 0.35$	0.77
Age (years)	42.17 ± 8.37	45.22 ± 9.71	t = 1.14	0.26
Education (years)	10.52 ± 3.50	11.83 ± 4.54	t = 1.09	0.28
VAS	7.04 ± 0.767	-	-	-
Duration of pain (months)	8.87 ± 4.83	-	-	-

Note: MFP, myofascial pain; HC, healthy controls; M/F, male/female; VAS, visual analog scale; Data are expressed as means ± SD.

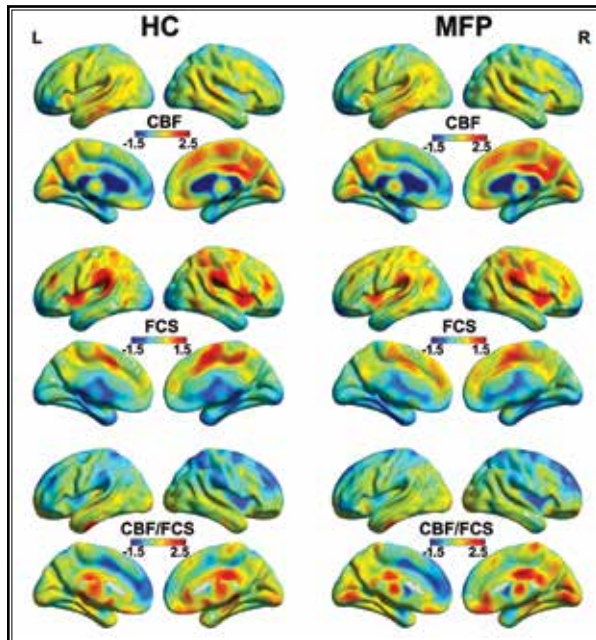


Fig. 1. Spatial distribution maps of CBF, FCS (at the threshold of 0.2), and CBF/FCS ratio in HC and patients with MFP. The CBF, FCS, and CBF/FCS ratio maps are normalized to z-scores and averaged across patients within groups. MFP, myofascial pain; HC, healthy controls; CBF, cerebral blood flow; FCS, functional connectivity strength; L, left; R, right.

pling alterations in patients with MFP, the intergroup comparisons of CBF/FCS ratios were repeated while controlling for the influence of GMV. After GMV corrections had been made, the spatial distribution of brain regions with significant differences in the CBF/FCS ratio was similar to the distribution obtained without GMV corrections (Fig. 6), suggesting that GMV atrophy did

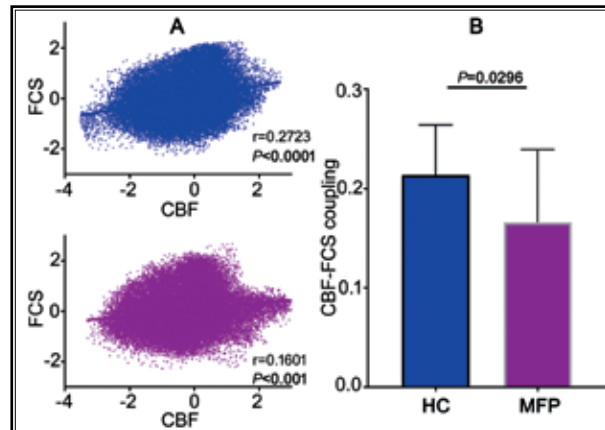


Fig. 2. CBF-FCS coupling changes in the whole gray matter in the patients with MFP. A: Scatter plots of the voxels spatial correlation between CBF and FCS in HC (blue) and patients with MFP (purple). B: Average CBF-FCS coupling in the whole gray matter in the patients with MFP and HC. Although CBF and FCS was significantly correlated in both groups, CBF-FCS coupling was significantly reduced in the patients with MFP compared with the HC, and a significant across-voxels difference in the CBF-FCS correlation coefficient was found between the patients with MFP and HC. Error bars represent the standard error. MFP, myofascial pain; HC, healthy controls; CBF, cerebral blood flow; FCS, functional connectivity strength.

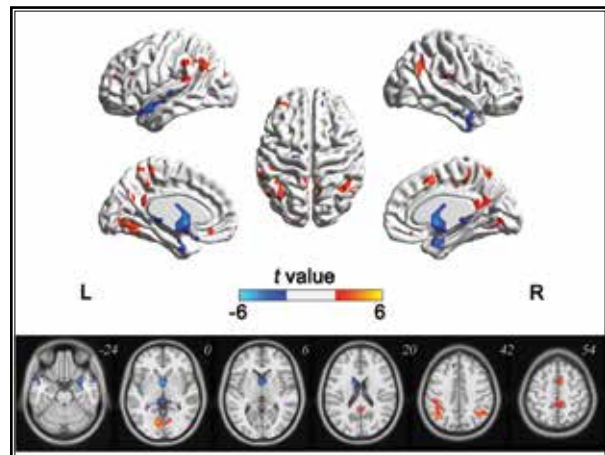


Fig. 3. Group differences in CBF/FCS ratio between patients with MFP and HC ( $P < 0.05$ , FDR corrected). The warm and cold colors indicate significantly increased and decreased CBF/FCS ratio in the patients with MFP, respectively. MFP, myofascial pain; HC, healthy controls; CBF, cerebral blood flow; FCS, functional connectivity strength; L, left; R, right.

not influence neurovascular coupling alterations in patients with MFP.

Table 2. Brain regions with significantly different CBF/FCS ratios between MFP and HC.

Regions	Brodmann areas	Cluster size (voxels)	Peak t values	Coordinates in MNI (x, y, z)
<b>MFP &lt; HC</b>				
Left superior temporal gyrus	22	120	-5.2	-54, 6, -18
Right superior temporal gyrus	22	134	-5.1	55, 6, -29
Right parahippocampal	35	89	-4.96	27, 6, -27
Right hippocampus	36	55	-4.85	22, -11, -11
Caudate		98	-5.25	-1, 5, 5
Superior frontal gyrus	9	165	-4.78	16, 44, 41
Periaqueductal		55	-4.46	7, -33, -3
<b>MFP &gt; HC</b>				
Left lingual gyrus	19	61	4.78	-9, -72, -3
Right lingual gyrus	19	42	4.25	6, -75, -3
Posterior cingulate	23	121	4.91	3, -50, 19
Left Inferior parietal lobule	40	220	4.98	-40, -63, 41
Right Inferior parietal lobule	40	258	5.36	54, -57, 33

Note: MFP, myofascial pain; HC, healthy controls; CBF, cerebral blood flow; FCS, functional connectivity strength; MNI, Montreal Neurological Institute.

## DISCUSSION

This study demonstrates for the first time that whole-brain gray matter CBF-FCS coupling was reduced and the CBF/FCS ratio of the PAG was significantly negatively correlated with pain VAS score and pain duration in patients with chronic MFP.

Although the CBF-FCS correlation could only roughly assess the neurovascular coupling, any changes in neurovascular coupling should be interpreted in terms of its structural basis. NVUs form the structural basis of neurovascular coupling, with the components of NVUs closely linked to one another and forming a complete functional and anatomical structure, which serves as a highly efficient CBF regulatory system (26). Damage to any of the components of an NVU may influence the normal functioning of the entire unit and ultimately result in neurovascular coupling disorders (21).

Alterations in the CBF of patients with MFP may be related to alterations in chronic pain modulation

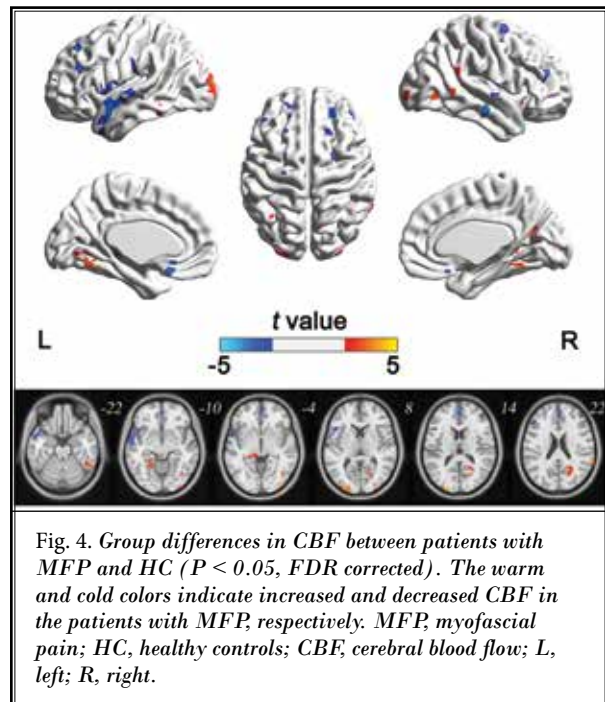


Fig. 4. Group differences in CBF between patients with MFP and HC ( $P < 0.05$ , FDR corrected). The warm and cold colors indicate increased and decreased CBF in the patients with MFP, respectively. MFP, myofascial pain; HC, healthy controls; CBF, cerebral blood flow; L, left; R, right.

Table 3. Brain regions with significantly different CBF between MFP and HC.

Regions	Brodmann areas	Cluster size (voxels)	Peak t values	Coordinates in MNI (x, y, z)
<b>MFP &lt; HC</b>				
Left superior temporal gyrus	22	165	-5.1	-54, 3, -10
Left middle temporal gyrus	21	143	-4.72	-60, -12, -20
Right midfrontal gyrus	10	104	-4.45	44, 45, 17
Medial frontal gyrus	9	148	-4.91	0, 56, 15
Periaqueductal grey matter		68	-4.23	2, -32, -7
Right superior temporal gyrus	22	86	-4.64	66, -19, -19
<b>MFP &gt; HC</b>				
Right Inferior temporal gyrus	20	102	4.35	49, -48, -20
Calcarine	17	112	4.93	22, -64, 20
Left parahippocampal	35	79	4.23	-23, -54, -10

Note: MFP, myofascial pain; HC, healthy controls; CBF, cerebral blood flow; MNI, Montreal Neurological Institute.

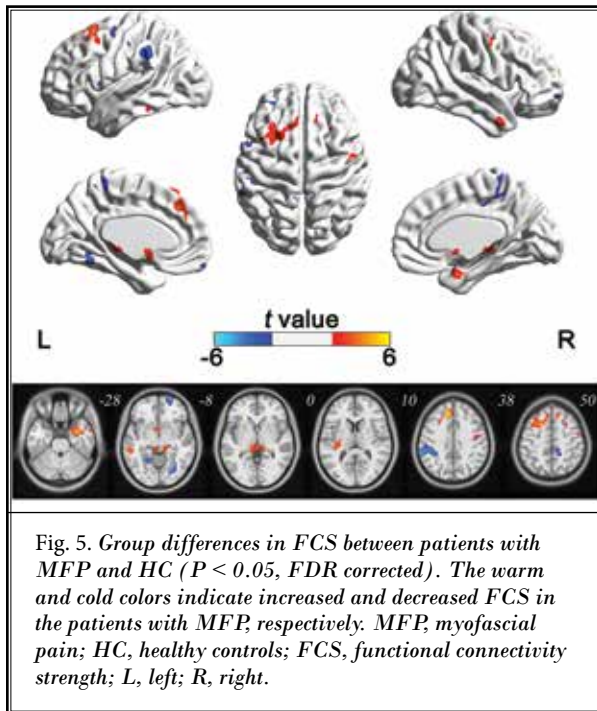


Table 4. Brain regions with significantly different FCS between MFP and HC.

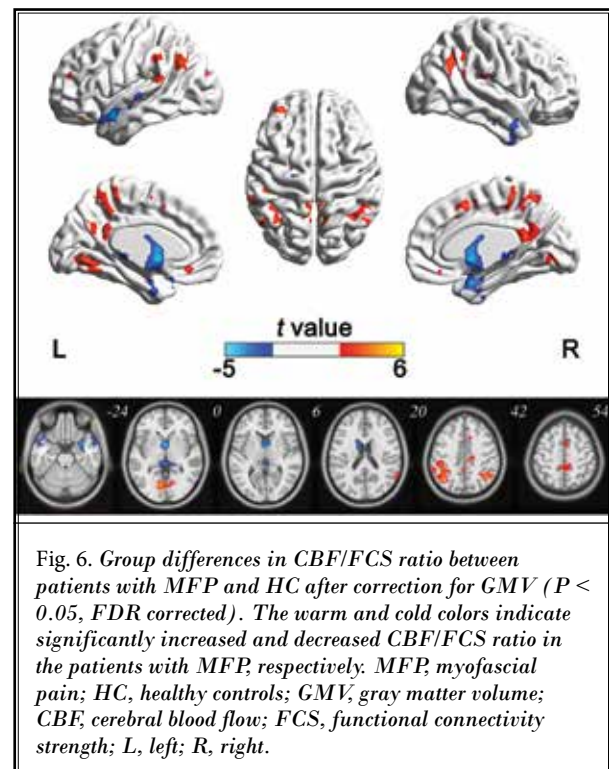
Regions	Brodmann areas	Cluster size (voxels)	Peak t values	Coordinates in MNI (x, y, z)
<b>MFP &lt; HC</b>				
Superior frontal gyrus	9	105	-5.18	21, 60, -9
Left insula	13	68	-4.37	-48, 6, 3
Left inferior parietal lobule	40	168	-4.6	-66, -39, 39
Left lingual gyrus	19	78	-4.32	-24, -57, -6
<b>MFP &gt; HC</b>				
Right temporal gyrus	22	136	4.9	33, 0, -27
Right para-hippocampal	35	78	4.76	26, -1, -29
Left middle temporal gyrus	21	106	5.12	-56, -36, -11
Periaqueductal		110	4.58	9, -34, -2
Left superior frontal gyrus	9	212	5.2	-21, 15, 56

Note: MFP, myofascial pain; HC, healthy controls; FCS, functional connectivity strength; MNI, Montreal Neurological Institute.

Table 5. Correlations between CBF/FCS ratio and clinical symptoms in patients with MFP.

Regions	VAS	Duration of pain
<b>MFP &lt; HC</b>		
Left superior temporal gyrus	0.287 (0.248)	0.198 (0.381)
Right superior temporal gyrus	0.162 (0.481)	0.231 (0.329)
Right parahippocampal	-0.375 (0.095)	-0.369 (0.102)
Right hippocampus	-0.416 (0.069)	-0.402 (0.078)
Caudate	-0.324 (0.135)	-0.301 (0.157)
Superior frontal gyrus	-0.421 (0.068)	-0.368 (0.104)
Periaqueductal	-0.505 (0.024)*	-0.493 (0.031)*
<b>MFP &gt; HC</b>		
Left lingual gyrus	0.161 (0.441)	0.155 (0.506)
Right lingual gyrus	0.148 (0.582)	0.167 (0.411)
Posterior cingulate	-0.375 (0.098)	-0.349 (0.123)
Left Inferior parietal lobule	0.281 (0.238)	0.234 (0.313)
Right Inferior parietal lobule	0.167 (0.443)	0.229 (0.319)

Note: MFP, myofascial pain; HC, healthy controls; VAS, visual analog scale; CBF, cerebral blood flow; FCS, functional connectivity strength. \*significant for  $p < 0.05$ .



systems such as the opioid, noradrenergic, 5-hydroxytryptamine systems and neuroplasticity markers (brain-derived neurotrophic factor) (27-30), as these chemical substances play a crucial role in the regulation of vascular responses. In addition, chronic pain may alter plasticity in neurons, leading to central sensitization and insufficient pain inhibition (31). Consequently, a compensatory mechanism is triggered, which induces arteriole vasodilation to meet local metabolic demands and ultimately results in CBF alterations. FCS describes the whole-brain functional connectivity of each voxel from a brain-wide network perspective and reflects the role of each voxel in the transfer of information across the entire network (13). The FCS alterations in patients with MFP may be the result of microstructural damage in the gray matter (10,11), and the loss of structural integrity may affect the precise coordination of functional synchronization among brain regions.

By contrast, the CBF/FCS ratio measures the blood supply to each FCS unit and reflects neurovascular coupling in a specific voxel or brain region (14). Compared with the CBF-FCS correlation, the CBF/FCS ratio provides a more detailed reflection of alterations in neurovascular coupling across the whole brain in patients with MFP. In the present study, it was found that, compared with the HC, the patients with MFP group had decreased CBF/FCS ratios in the bilateral superior temporal gyri, right parahippocampal gyrus, right hippocampus, right caudate nucleus, right medial prefrontal cortex, and PAG and increased CBF/FCS ratios in the bilateral lingual gyri, posterior cingulate cortex, and bilateral inferior parietal lobules. These results indicate that neurovascular coupling alterations occurred in the aforementioned brain regions of patients with MFP. During the validation analysis, we confirmed that changes in the CBF/FCS ratio were not associated with gray matter atrophy, which provides further proof that brain regions with neurovascular coupling abnormalities are reliable indicators of MFP.

In patients with MFP, significant changes occurred in the CBF/FCS ratios of the posterior cingulate cortex, medial prefrontal cortex, and inferior parietal lobule, which are key components of the default mode network. As the posterior cingulate cortex is directly or indirectly linked to a large number of nuclei in the cerebral cortex and subcortex through fiber connections, it may possibly play a pivotal role in the integration, memory formation, and execution of pain sensations (32). In a study by Flodin et al (33), abnormalities were found in the functional connectivity between multiple brain regions

and the cingulate cortex in patients with chronic pain, which may be associated with persistent pain stimuli. The inferior parietal lobule is involved in memory formation, sorting, and storage (34) and may be closely linked to the alleviation of pain. The medial prefrontal cortex can inhibit the input of nociceptive signals (35), which leads to the generation of inhibitory effects in the brain region upon the receipt of pain signals and influences the cognitive function of patients through interactions with neighboring brain regions (36). In addition, it was found that changes occurred in the CBF/FCS ratios of the parahippocampal gyrus, hippocampus, and PAG of patients with MFP. These brain regions constitute the limbic system and are closely associated with emotional responses to pain. Therefore, our results suggest that neurons of the default mode network and limbic system are more prone to damage, which may explain the presence of abnormalities in the sensation, integration, and emotional responses of pain in patients with MFP.

In this study we also observed that the CBF/FCS ratio of the PAG was negatively correlated with VAS and pain duration. The PAG is a key component of descending pain modulation and networks related to the receipt of input from noxious stimulation (37,38) and plays an important role in pain occurrence and modulation. In a cold pressor test conducted in another study, it was observed that PAG activation was positively correlated with pain threshold but negatively correlated with perceived pain intensity (39). Other researchers reported that the pain duration and pain scores of patients with chronic low back pain were negatively correlated with PAG functional connectivity (40). Our data indicate that pain duration and intensity play a crucial role in neurovascular coupling alterations in patients with chronic MFP, with PAG neurons being more easily influenced by these factors.

### Limitations

Alterations in neurovascular coupling in patients with MFP were observed only before treatment. Therefore, there is a lack of data on the alterations that occurred after treatment.

### CONCLUSION

This study demonstrated for the first time that impairment of neurovascular coupling in the brain may be a potential neuropathological mechanism of chronic MFP.

### Acknowledgments

The author thanks the patients and all the members of their families.

## REFERENCES

- Xie P, Qin B, Yang F, et al. Lidocaine injection in the intramuscular innervation zone can effectively treat chronic neck pain caused by MTrPs in the trapezius muscle. *Pain Physician* 2015; 18:E815-E826.
- Park CH, Lee YW, Kim YC, Moon JH, Choi JB. Treatment experience of pulsed radiofrequency under ultrasound guided to the trapezius muscle at myofascial pain syndrome -A case report-. *Korean J Pain* 2012; 25:52-54.
- Graboski CL, Gray DS, Burnham RS. Botulinum toxin A versus bupivacaine trigger point injections for the treatment of myofascial pain syndrome: A randomized double blind crossover study. *Pain* 2005; 118:170-175.
- Borg-Stein J, Iaccarino MA. Myofascial pain syndrome treatments. *Phys Med Rehabil Clin N Am* 2014; 25:357-374.
- De Andrés J, Cerda-Olmedo G, Valía JC, Monsalve V, Lopez-Alarcón, Minguez A. Use of botulinum toxin in the treatment of chronic myofascial pain. *Clin J Pain* 2003; 19:269-275.
- Fernández-de-las-Peñas C, Dommerholt J. Myofascial trigger points: Peripheral or central phenomenon? *Curr Rheumatol Rep* 2014; 16:395.
- Shokouhi M, Clarke C, Morley-Forster P, Moulin DE, Davis KD, St Lawrence K. Structural and functional brain changes at early and late stages of complex regional pain syndrome. *J Pain* 2018; 19:146-157.
- Harper DE, Ichescio E, Schrepf A, et al. Relationships between brain metabolite levels, functional connectivity, and negative mood in urologic chronic pelvic pain syndrome patients compared to controls: A MAPP research network study. *Neuroimage Clin* 2017; 17:570-578.
- Kutch JJ, Labus JS, Harris RE, et al. Resting-state functional connectivity predicts longitudinal pain symptom change in urologic chronic pelvic pain syndrome: A MAPP network study. *Pain* 2017; 158:1069-1082.
- Niddam DM, Lee SH, Su YT, Chan RC. Brain structural changes in patients with chronic myofascial pain. *Eur J Pain* 2017; 21:148-158.
- Xie P, Qin B, Song G, et al. Microstructural abnormalities were found in brain gray matter from patients with chronic myofascial pain. *Front Neuroanat* 2016; 10:122.
- Niddam DM, Chan RC, Lee SH, Yeh TC, Hsieh JC. Central representation of hyperalgesia from myofascial trigger point. *Neuroimage* 2008; 39:1299-1306.
- Gao Q, Xu F, Jiang C, et al. Decreased functional connectivity density in pain-related brain regions of female migraine patients without aura. *Brain Res* 2016; 1632:73-81.
- Liang X, Zou Q, He Y, Yang Y. Coupling of functional connectivity and regional cerebral blood flow reveals a physiological basis for network hubs of the human brain. *Proc Natl Acad Sci U S A* 2013; 110:1929-1934.
- Tomasi D, Wang GJ, Volkow ND. Energetic cost of brain functional connectivity. *Proc Natl Acad Sci U S A* 2013; 110:13642-13647.
- Vaishnavi SN, Vlassenko AG, Rundle MM, Snyder AZ, Mintun MA, Raichle ME. Regional aerobic glycolysis in the human brain. *Proc Natl Acad Sci U S A* 2010; 107:17757-17762.
- Paulson OB, Hasselbalch SG, Rostrup E, Knudsen GM, Pelligrino D. Cerebral blood flow response to functional activation. *J Cereb Blood Flow Metab* 2010; 30:2-14.
- Keszthelyi D, Aziz Q, Ruffle JK, et al. Delineation between different components of chronic pain using dimension reduction - an ASL fMRI study in hand osteoarthritis. *Eur J Pain* 2018; 22:1245-1254.
- Phillips AA, Chan FH, Zheng MM, Krassioukov AV, Ainslie PN. Neurovascular coupling in humans: Physiology, methodological advances and clinical implications. *J Cereb Blood Flow Metab* 2016; 36:647-664.
- Muoio V, Persson PB, Sendeski MM. The neurovascular unit - concept review. *Acta Physiol (Oxf)* 2014; 210:790-798.
- Zlokovic BV. Neurodegeneration and the neurovascular unit. *Nat Med* 2010; 16:1370-1371.
- Kuschinsky W. Coupling of function, metabolism, and blood flow in the brain. *Neurosurg Rev* 1991; 14:163-168.
- Zhu J, Zhuo C, Xu L, Liu F, Qin W, Yu C. Altered coupling between resting-state cerebral blood flow and functional connectivity in schizophrenia. *Schizophr Bull* 2017; 43:1363-1374.
- Xu G, Rowley HA, Wu G, et al. Reliability and precision of pseudo-continuous arterial spin labeling perfusion MRI on 3.0 T and comparison with 15O-water PET in elderly subjects at risk for Alzheimer's disease. *NMR Biomed* 2010; 23:286-293.
- Saxena N, Gili T, Diukova A, Huckle D, Hall JE, Wise RG. Mild propofol sedation reduces frontal lobe and thalamic cerebral blood flow: An arterial spin labeling study. *Front Physiol* 2019; 10:1541.
- Armstead WM, Raghupathi R. Endothelin and the neurovascular unit in pediatric traumatic brain injury. *Neuro Res* 2011; 33:127-132.
- Taylor BK, Fu W, Kuphal KE, et al. Inflammation enhances Y1 receptor signaling, neuropeptide Y-mediated inhibition of hyperalgesia, and substance P release from primary afferent neurons. *Neuroscience* 2014; 256:178-194.
- Martins I, Carvalho P, de Vries MG, et al. Increased noradrenergic neurotransmission to a pain facilitatory area of the brain is implicated in facilitation of chronic pain. *Anesthesiology* 2015; 123:642-653.
- Ossipov MH, Morimura K, Porreca F. Descending pain modulation and chronification of pain. *Curr Opin Support Palliat Care* 2014; 8:143-151.
- Trang T, Beggs S, Salter MW. Brain-derived neurotrophic factor from microglia: A molecular substrate for neuropathic pain. *Neuron Glia Biol* 2011; 7:99-108.
- Latremoliere A, Woolf CJ. Central sensitization: A generator of pain hypersensitivity by central neural plasticity. *J Pain* 2009; 10:895-926.
- Vincent JL, Kahn I, Snyder AZ, Raichle ME, Buckner RL. Evidence for a frontoparietal control system revealed by intrinsic functional connectivity. *J Neurophysiol* 2008; 100:3328-3342.
- Flodin P, Martinsen S, Mannerkorpi K, et al. Normalization of aberrant resting state functional connectivity in fibromyalgia patients following a three month physical exercise therapy. *Neuroimage Clin* 2015; 9:134-139.
- Banks SJ, Eddy KT, Angstadt M, Nathan PJ, Phan KL. Amygdala-frontal connectivity during emotion regulation. *Soc Cogn Affect Neurosci* 2007; 2:303-312.
- Tessitore A, Russo A, Giordano A, et al. Disrupted default mode network connectivity in migraine without aura. *J Headache Pain* 2013; 14:89.
- Mainero C, Boshyan J, Hadjikhani N. Altered functional magnetic resonance

- imaging resting-state connectivity in periaqueductal gray networks in migraine. *Ann Neurol* 2011; 70:838-845.
37. Keya KA, Bandler R. Distinct central representations of inescapable and escapable pain: Observations and speculation. *Exp Physiol* 2002; 87:275-279.
38. Lumb BM. Hypothalamic and midbrain circuitry that distinguishes between escapable and inescapable pain. *News Physiol Sci* 2004; 19:22-26.
39. La Cesa S, Tinelli E, Toschi N, et al. fMRI pain activation in the periaqueductal gray in healthy volunteers during the cold pressor test. *Magn Reson Imaging* 2014; 32:236-240.
40. Yu R, Gollub RL, Spaeth R, Napadow V, Wasan A, Kong J. Disrupted functional connectivity of the periaqueductal gray in chronic low back pain. *Neuroimage Clin* 2014; 6:100-108.